Demonstration of a Room-Temperature Single-Photon Source for Quantum Information: Single-Dye-Molecule Fluorescence in a Cholesteric Liquid Crystal Host

Introduction

Quantum information in the form of quantum communications and quantum computing (see Refs. 1–33) is currently an exceedingly active field. Numerous theoretical concepts promise powerful quantum-mechanics-based tools[34] that, to date, wait for realization pending the arrival of reliable hardware.[1–33] A *single-photon source* (SPS)[35] that efficiently produces photons with *antibunching* characteristics[36–38] is one such pivotal hardware element for quantum information technology. Using an SPS, secure quantum communication will prevent any potential eavesdropper from intercepting a message without the receiver noticing.[25,30,39–41] In another implementation, an SPS becomes the key hardware element for quantum computers with linear optical elements and photodetectors.[42–52] Again, its practical realization is held back in part because of the difficulties in developing robust sources of antibunched photons on demand. In spite of several solutions for SPS's presented in the literature, significant drawbacks remain. The drawbacks are the reason for current quantum communication systems being baud-rate bottlenecked, causing photon numbers from ordinary photon sources to attenuate to the single-photon level (~0.1 photon per pulse on average).[25,39,41] An efficient (with an-order-of-magnitude-higher photon number per pulse) and reliable light source that delivers a train of pulses containing one, and only one, photon is a very timely challenge. To meet this challenge, several issues need to be addressed, from achieving full control of the quantum properties of the source to easy handling and integrability of these properties in a practical quantum computer and/or communication setup. In addition, in quantum information systems it is desirable to deal with single photons synchronized to an external clock, namely, *triggerable* single photons.[53] *Polarization states* of single photons are also important since they enable polarization-qubit encoding of information.

The critical issue in producing single photons in another way than by trivial attenuation of a beam is the *very low concentration of photon emitter*s dispersed in a host, such that within a laser focal spot only one emitter becomes excited, emitting only one photon at a time. In initial demonstrations of resonance-fluorescence photon antibunching,[54] SPS's possessed a random photon-emission time.[54–63] Single photons "on demand," i.e., triggerable single photons, were obtained only recently.[53,64–76] De Martini *et al.*[64] used an active microcavity excited by a mode-locked laser. In experiments by Kim *et al.*,[65] Imamoglu *et al.*,[66] and Moreau *et al.*,[67] a single-photon turnstile device utilized Coulomb blockade of tunneling for electrons and holes in a mesoscopic double-barrier *p–n* junction. Single photons were generated at the modulation periodicity of the junction voltage. Michler *et al.*[68] and Santory *et al.*[69] demonstrated single-photon devices using pulsed-laser excitation of a single AlGaAs quantum dot. Electrically driven single photons (also at cryogenic temperatures as in Refs. 65–69) were obtained by Yuan *et al.*[70,71] Experiments by Brunel *et al.*,[72] Lounis and Moerner,[73] and Treussart *et al.*[74] were based on an entirely different system, namely single dye molecules embedded at low concentration within organic single-crystal platelets or covered by a polymer layer. Single photons were triggered either by a combination of cw laser excitation and an electronic signal[72] or by short-pulse laser irradiation.[73,74] Most of these sources, e.g., Refs. 65–71, operate reliably only at liquid He temperature—a major impediment to widespread use. To date, three approaches are known to be eligible for *room-temperature* SPS implementation, two inorganic and one organic. The first inorganic, room-temperature approach involves a mono-/polycrystal diamond and one of its color centers.[59–61,75,76] The second inorganic approach uses single-colloidal CdSe/ZnS quantum dots (Michler *et al.*,[77] Lounis *et al.*,[78] and Messin *et al.*[79]). The alternative, organic approach,[58,62,63,72–74] based on numerous previous experiments around liquid-He temperature,[80–83] uses a vapor-phase-sublimated host crystal of para-terphenyl doped with an emitting species, terrylene.[62,73]

As acceptable as these approaches may be strictly on quantum-optics grounds, all suffer from shortcomings that will delay quantum information from gaining a technology foothold in the near future. None of these sources is used in practical, civilian systems. Their specific shortcomings include the following: (1) Polarization of single photons varies

from one emitter to another (nondeterministic); (2) single photons are produced with *very low efficiency* and *polluted* by additional photons at about the same frequency from the host material;[53] and (3) alternatives such as color centers in diamond and colloidal CdSe/ZnS quantum dots possess unacceptably long fluorescence lifetimes (for instance, the diamond color center has a 11.6-ns and 22.7-ns fluorescence lifetime in mono- and polycrystal, and CdSe-ZnS quantum dots have a fluorescence lifetime of ~22 ns).

The organic, room-temperature SPS approach is based on using a chromophore molecule as the single emitter. The key advantage of chromophore molecules is that their excited-state lifetime of only a few nanoseconds permits excitation repetition rates above ~100 MHz. In *amorphous* media such molecules tend to be *unstable*: they are blinking at various characteristic time intervals, change their spectral behavior, and can be easily bleached. Recently, however, single terrylene molecules have been doped into *p*-terphenyl molecular *crystals* (10^{-11} moles of terrylene per mole of *p*-terphenyl) prepared by a sublimation procedure that produced tiny platelets.[62,73] In this host, the chromophore is protected from exposure to diffusing quenchers (such as oxygen) and benefits from strong phonon emission into the host, preventing rapid thermal decomposition of the chromophore under intense irradiation. In Ref. 73 it was found that for "thick" *p*-terphenyl crystals (~10 μm), this system becomes extremely photostable, allowing hours of continuous illumination of individual molecules without photobleaching. It assures long-term spectral stability and reproducibility from one terrylene absorber to the next.[84,85] Pumped by periodic, short-pulse laser radiation, single photons were generated at predetermined times at pump-pulse-repetition rates within the accuracy of the emission lifetime (~3.8 ns). Technical implementation of this system is difficult because these monoclinic, sublimation-produced microcrystals are stress sensitive and fragile. In addition, terrylene's molecular dipole moment in the *p*-terphenyl host crystal takes on an orientation perpendicular to the platelet's surface (i.e., perpendicular to the incident light's E field).[73] This, in turn, leads to poor coupling with the polarized excitation light, prompting poor fluorescence emission even at high excitation intensities (saturation intensity is about 1 MW/cm^2 at room temperature). In spite of the elegance of the terrylene/*p*-terphenyl experiments, this technology must be considered unrealistic for practical application. Its weak point is also a background from "ordinary photons" from out-of-focus molecules or Raman scattering because of the very high pumping intensities required. Emitted photons are not polarized *deterministically* (there is no known efficient method for aligning rapidly a multitude of micrometer-sized, monoclinic crystallites relative to one another). Note that noncrystalline, amorphous hosts, e.g., polymers,[63] neither (1) offer the same spectral stability in single-molecule emission even in the case of terrylene, nor (2) provide long-time protection against bleaching. To date, *no crystal hosts* other than the fragile, sublimated *p*-terphenyl flakes have been proposed in *single-molecule room-temperature* experiments.

This article describes some new approaches toward implementing an efficient, deterministically polarized SPS on demand: (1) using *liquid crystal hosts* (including liquid crystal polymers) to preferentially align the emitter molecules for maximum excitation efficiency (deterministic molecular alignment will also provide deterministically polarized output photons); (2) using planar-aligned cholesteric (chiral-nematic) liquid crystal hosts[86] as 1-D photonic-band-gap microcavities[87–91] tunable to the dye fluorescence band;[92–93] and (3) using liquid crystal technology to prevent dye bleaching.

Cholesteric-Liquid-Crystal, 1-D Photonic-Band-Gap Materials

In planar cholesterics (Fig. 94.24) that for visualization purposes can be described as consisting of, but in reality not comprising, a layered structure, the axes of the molecular director (far-right set of arrows in Fig. 94.24) rotate monotonically to form a periodic helical structure with pitch P_0.[86] With few exceptions, liquid crystal media are non-chiral and require

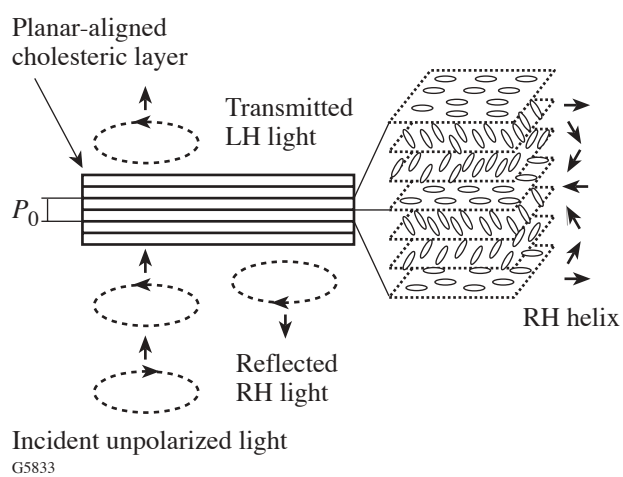

Figure 94.24
Transmission and reflection by a cholesteric liquid crystal layer near selective reflection conditions.

additives to induce the chiral order. Dependent on the chirality-inducing additive, the final structure may show either a right- or a left-handed sense of rotation.

When a solid cholesteric is flipped on its side and inspected by a high-resolution tool such as an atomic force microscope, the periodic pitch becomes observable through height variations along the helical axis. For instance, Fig. 94.25 shows such a topography for a Wacker cyclo-tetrasiloxane-oligomer cholesteric liquid crystal (OCLC)[94] platelet. Periodic stripes in the image correspond to one-half of the pitch length.

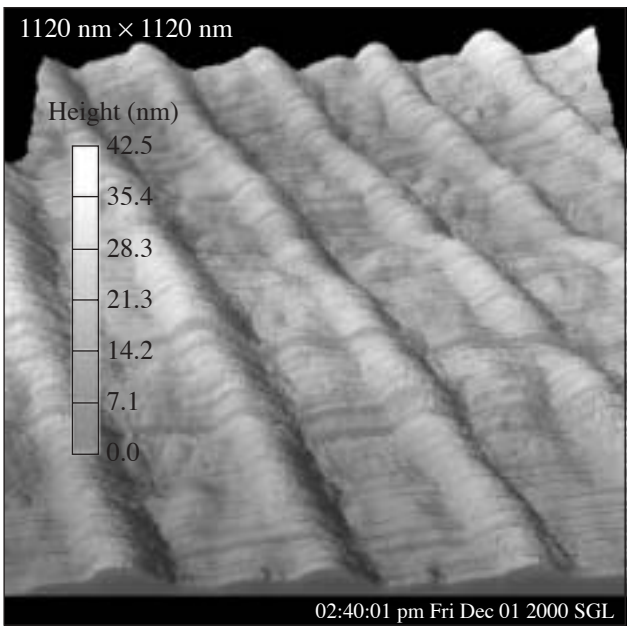

G5834

Figure 94.25
Perspective view of the AFM topographical image of a planar-aligned Wacker OCLC layer (1.12-μm × 1.12-μm scan).

For liquid crystal thicknesses ≥10 μm, the reflectance of normally incident, circularly polarized light with electric-field vector rotation opposite to the rotation of molecules in the helical structure (Bragg condition) approaches 100% within a band centered at $\lambda_0 = n_{av}P_0$, where $n_{av} = (n_e + n_0)/2$ is the average of the ordinary and extraordinary refractive indices of the medium. This is the so-called selective reflection of cholesteric liquid crystals. The bandwidth is $\Delta\lambda = \lambda_0 \Delta n / n_{av}$, where $\Delta n = n_e - n_0$. Such a periodic structure can also be viewed as a 1-D photonic crystal, with a bandgap within which propagation of light is forbidden. For emitters located within such a structure, the rate of spontaneous emission is suppressed within the spectral stop band and enhanced near the band edge.[95] Several groups have reported lasing in photonic bandgap material hosts, including cholesteric liquid crystals,[95–98] with spectral emission features underscoring the validity of this concept. Generation of strongly circularly polarized photoluminescence from planar layers of glass-forming chiral-nematic liquid crystals was also reported.[92–93] Light-emitting dopants at 0.2-wt% concentration were embedded in these liquid crystals. The degree of circularly polarized photoluminescence, i.e., its asymmetry,[92–93]

$$G_e \equiv 2(I_L - I_R)/(I_L + I_R), \tag{1}$$

where I_R and I_L denote the right- and left-handed emission intensity, respectively (see Fig. 94.26), was found to be equal to maximum value [~ −2 (Refs. 92 and 93)].

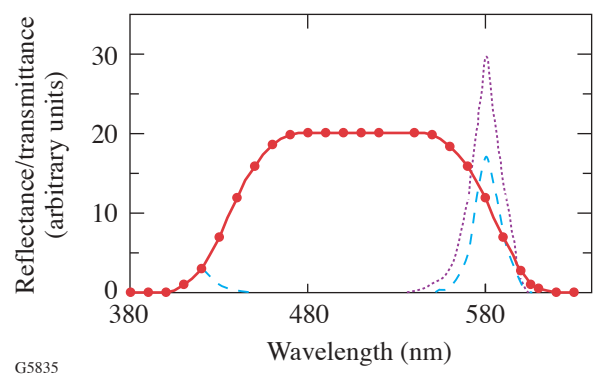

G5835

Figure 94.26
Tutorial schematic of the wavelength dependence between the photonic stop-band reflectance (solid line), dye photoluminescence intensity (dotted line), and photoluminescence polarization asymmetry G_e inside the band (dashed line).

Matching of λ_0 of cholesteric liquid crystal with a dye-fluorescence band will be the subject of a future article. In our current experiments, Wacker OCLC (see Fig. 94.27) with λ_0 outside the terrylene-dye-fluorescence band was doped with terrylene (Fig. 94.28) at an extremely low concentration such that the final sample contained only a few molecules per μm^2 irradiation area. Cast from solution on single microscope cover-glass slips, the samples ranged in thickness from ~50 nm to several micrometers. In some experiments, we also used terrylene-doped layers of monomeric cyanobiphenyl liquid crystal 5CB with chiral additive CB15. The 5CB liquid crystal layers were placed between two microscope cover-glass slips separated by glass-bead spacers.

To minimize false fluorescence contributions by contaminants during single-molecule-fluorescence microscopy, rigorous cleaning of glass substrates is mandatory. For this purpose, the microscope glass slips (Corning, 0.17-mm thickness) were etched in a piranhas solution and rinsed in deionized water. Proper terrylene concentration for single-molecule fluorescence microscopy was established by iterative trial and error. In sequential dilution steps of terrylene in chlorobenzene solvent, solutions were spun onto glass slips, and for each concentration, confocal fluorescence microscopy determined the final emitter concentration per irradiation volume. Once single molecules were predominantly observed, the dilution endpoint was reached. This final terrylene solution was mixed with Wacker OCLC starting material (8% weight concentration of oligomer). For planar alignment, standard buffing procedures could not be employed at the risk of introducing dirt particles. Two alternate methods were found satisfactory: either the film was *flow aligned* by letting the OCLC solution run down a vertically inclined glass slip, or a special glass cylinder was rolled unidirectionally across a spin-coated OCLC layer heated to the isotropic state. Figure 94.29 shows an optical microscope image of a planar-aligned OCLC layer with "oily streak" defects typical for a planar structure of cholesteric liquid crystals (both monomeric and oligomeric/polymeric).[99–101] The influence of the oily streak defects on a single-molecule fluorescence will be considered in future work. We mention them here to show evidence of a planar structure of OCLC prepared by our group.

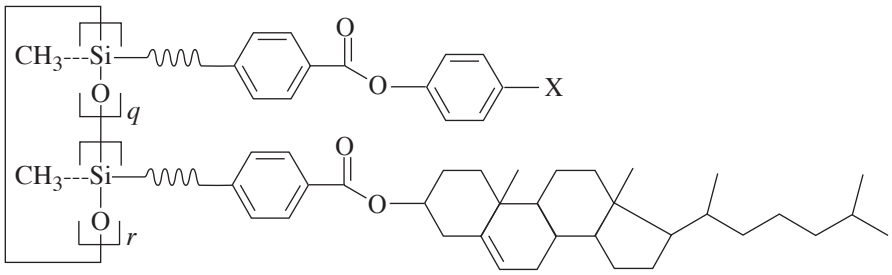

Figure 94.27
Molecular structure of Wacker siloxane OCLC (from Ref. 94).

$\sim\sim\sim\sim$ = —$(CH_2)_m$—$(O)_n$,

where m = 3, 4, 5, 6, 8, 10 and n = 0, 1;

$q + r$ = 3, 4, 5, 6, or 7 and $q/(q + r)$ = 0 to 1

X = Cl, OMe, $O(CH_2)_3H$, 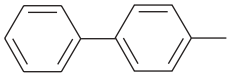 CN or 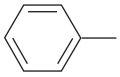 $(CH_2)_pH$, where p = 2, 4, or 5

G5836

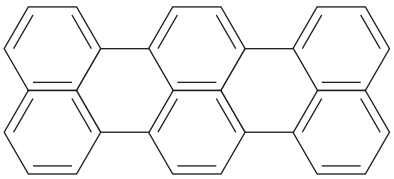

G5837

Figure 94.28
Molecular structure of terrylene dye.

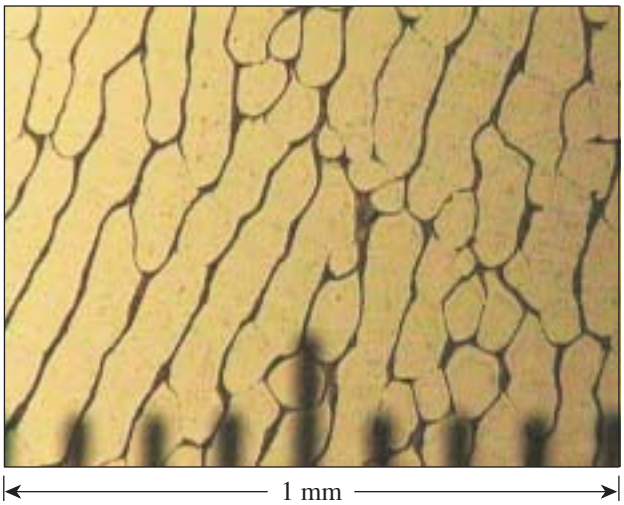

G5838

Figure 94.29
Optical microscopy of "oily streak" defects of planar-aligned Wacker OCLC layer.

Experimental Setup for Single-Dye-Molecule Fluorescence Microscopy and Antibunching Correlation Measurements

Photon antibunching correlation measurements are carried out using the setup shown in Figs. 94.30 and 94.31. The terrylene-doped liquid crystal sample is placed in the focal plane of a 0.8-N.A. microscope objective (Witec alpha-SNOM platform). The sample is attached to a piezoelectric, XYZ translation stage. Light emitted by the sample is collected by a confocal setup using a 1.25-N.A., oil-immersion objective together with an aperture formed by the core of a multimode optical fiber. The cw, spatially filtered (through a single-mode fiber), linearly polarized (contrast 10^5:1), 532-nm diode-pumped Nd:YAG laser output excites single molecules. In focus, the intensities used are of the order of several kW/cm^2. The collection fiber is part of a non-polarization-sensitive 50:50 fiber splitter that forms the two arms of a Hanbury Brown and Twiss correlation setup[102] (Fig. 94.31). Residual, transmitted excitation light is removed by two consecutive dielectric interference filters yielding a combined rejection of better than six orders of magnitude at 532 nm. The fluorescence band maximum of terrylene molecules used in our experiments lies in a spectral region near 579 nm with a bandwidth of ~30 nm.

G5839

Figure 94.30
Witec alpha-SNOM microscope with a laser.

Photons in the two Hanbury Brown and Twiss arms are detected by identical, cooled avalanche photodiodes in single-photon-counting Geiger mode. The time interval between two consecutively detected photons in separate arms is measured by a 68-ns-full-scale time-to-digital converter using a conventional start–stop protocol. Within this converter's linear range, the time uncertainty in each channel corresponds to 25 ps.

It has been proven experimentally (see, e.g., Refs. 62 and 63) that a very good approximation of the autocorrelation function $g^{(2)}(\tau)$ comes directly from the coincidence counts (event distribution) $n(\tau)$, for relatively low detection efficiency and therefore low counting rate. That is why we consider that $n(\tau)$ is proportional to the autocorrelation function $g^{(2)}(\tau)$. For single photons, $g^{(2)}(0) = 0$, indicating the absence of pairs, i.e., antibunching.

Experimental Results

1. Single-Dye-Molecule Fluorescence in a Cholesteric Liquid Crystal Host

Figure 94.32 shows terrylene-dye-molecule-fluorescence images obtained by confocal fluorescence microscopy: (a) single terrylene molecules embedded in a Wacker OCLC host (λ_0 = 2.2 μm); (b) clusters of terrylene molecules spin

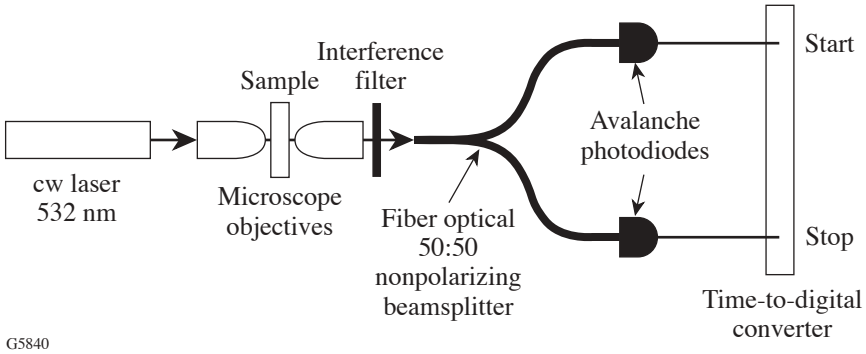

Figure 94.31
Experimental setup for photon antibunching correlation measurements.

coated from chlorobenzene solution onto a bare cover-glass slip. For both images, the scan direction is from left to right and line by line from top to bottom. The scan dimensions are 10 μm × 10 μm. Most single molecules in our samples exhibited fluorescence blinking in time, with a period ranging from several milliseconds up to several seconds. In Fig. 94.32, this "blinking" behavior by single molecules manifests itself as bright and dark horizontal stripes in image (a). These features are absent in emission images from clusters (b).

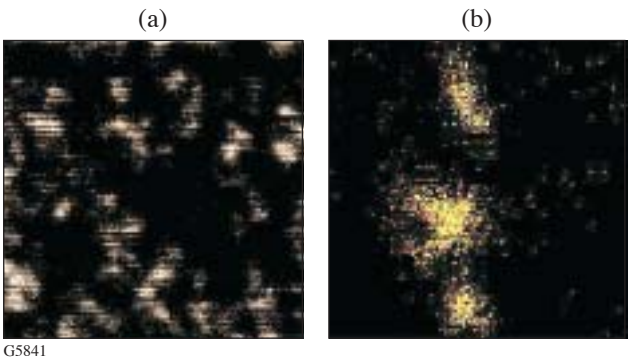

Figure 94.32
Terrylene molecule fluorescence: (a) single-molecule fluorescence from the OCLC host; (b) fluorescent-molecule clusters on a bare surface. Resolution of the optical system is ~0.5 μm.

Blinking is a common phenomenon and convincing evidence of the single-photon nature of the source. Several mechanisms are suggested to explain the blinking behavior: for instance, "shelving" (triplet blinking) to the long-living state, and fluctuations in the photo-physical parameters of the molecule and its local environment.[103] By modeling the molecule as a three-level system (singlet ground state S_0, excited-state level S_1, and triplet state T_1) as depicted in Fig. 94.33, "triplet blinking" can be explained by a population of T_1 level that is often a dark state in fluorescent dyes.

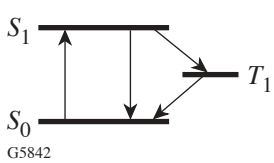

Figure 94.33
Three-level model for molecular fluorescence.

2. Photon Antibunching Correlation Measurements

Figure 94.34 shows a coincidence-count histogram $n(\tau)$ from (a) host-free single terrylene molecules (left) and (b) an assembly of many uncorrelated molecules within the excitation volume [Fig. 94.32(b)]. The scan speed is ~3 s per line (512 pixels). The left histogram exhibits a dip at $\tau = 0$. The measured signal-to-background ratio of our experiments ranges from 2 to 30, so the probability that a photon from the background triggers a coincidence with a photon from the molecule is very low. Because $n(\tau)$ is proportional to the autocorrelation function $g^{(2)}(\tau)$, $n(0) \sim 0$ means that $g^{(2)}(0) \sim 0$ in our experiments. Two fluorescence photons are not observed within an arbitrarily short time interval. This fluorescence antibunching is due to the finite radiative lifetime of the molecular dipole and is therefore clear proof that we observed the emission of one, and only one, molecule. The histogram on the right from a multiple of uncorrelated molecules shows no such dip at $\tau = 0$, i.e., no antibunching.

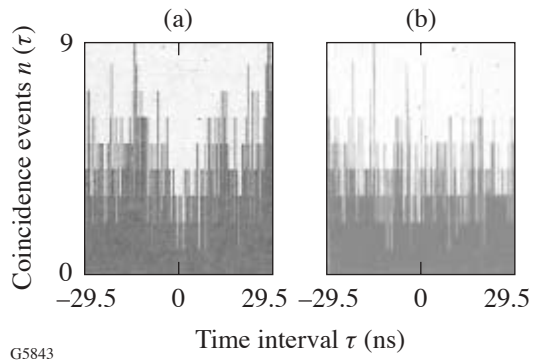

Figure 94.34
Histograms of concidence events of single-terrylene-molecule fluorescence on a bare glass substrate (a) and from an assembly of several uncorrelated molecules within the excitation volume (b).

To eliminate any potential for leaked excitation light causing the dip at $\tau = 0$, the sample was replaced with a bare glass slide and one blocking interference filter was removed. The coincidence histogram for this condition is depicted in Fig. 94.35(b). No antibunching is observed. Two interference filters attenuated excitation light so strongly that no counts other than dark counts of avalanche photodiodes were observed during the same time interval.

Figure 94.36 shows the results of doping terrylene into liquid crystals. The histogram of coincidence events $n(\tau)$ [Fig. 94.36(a)] exhibits a dip at $\tau = 0$ indicating photon antibunching in the fluorescence of the single molecules in the Wacker OCLC host; no antibunching is observed in the fluorescence from an assembly of several uncorrelated molecules in the same host, different sample [Fig. 94.36(b)]. The histogram in Fig. 94.36(a) is noteworthy in that it demonstrates that

several *single* molecules can sequentially contribute to an antibunching histogram without loss of $\tau = 0$ contrast, as in practice the long integration time and competing molecule-bleaching events make obtaining an entire, good-contrast histogram from only one molecule too much a matter of luck. When the initial single molecule was bleached, the sample was advanced to another single molecule while the photon-correlation count continued. This finding is crucial for future device implementation.

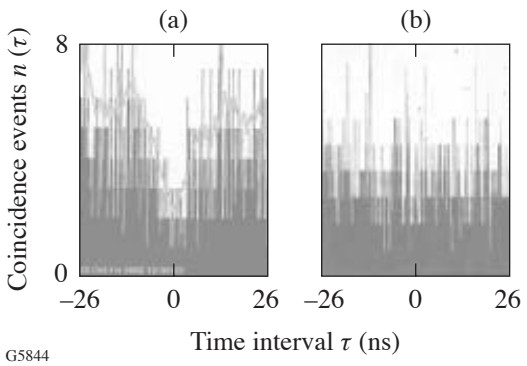

Figure 94.35
The histograms of concidence events of the single-terrylene-molecule fluorescence on a bare glass substrate (a) and of the radiation of excited green laser beam (b).

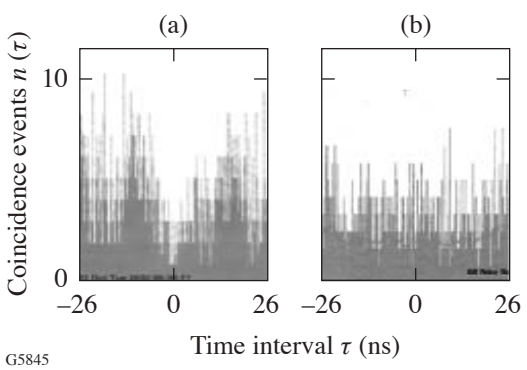

Figure 94.36
The histograms of concidence events of the single-terrylene-molecule fluorescence in a Wacker OCLC host (a) and of an assembly of several uncorrelated molecules (b).

3. Preventing Dye Bleaching in Liquid Crystal Hosts

Practical device implementation also depends on photochemical stability of both emitters and hosts. We increased terrylene fluorescence stability in monomeric liquid crystal hosts by saturating the liquid crystals with helium in a sealed glovebox for 1 h. Oxygen, which is mostly responsible for dye bleaching, is displaced by helium during this procedure. Ground-state oxygen can form highly reactive singlet oxygen by quenching a triplet state of the dye. The singlet oxygen can then react with its surroundings, including dye molecules. Figure 94.37 shows fluorescence-bleaching results of terrylene molecules at two-orders-of-magnitude-higher concentration than in single-molecule experiments in different liquid crystal hosts: either immobilized in an oligomer cholesteric liquid crystal or dissolved in monomeric cyanobiphenyl 5CB saturated with helium (both at identical excitation intensity and identical terrylene volume concentration). Over the course of more than 1 h, *no* dye bleaching was observed in the *oxygen-depleted* liquid crystal host (upper curve).

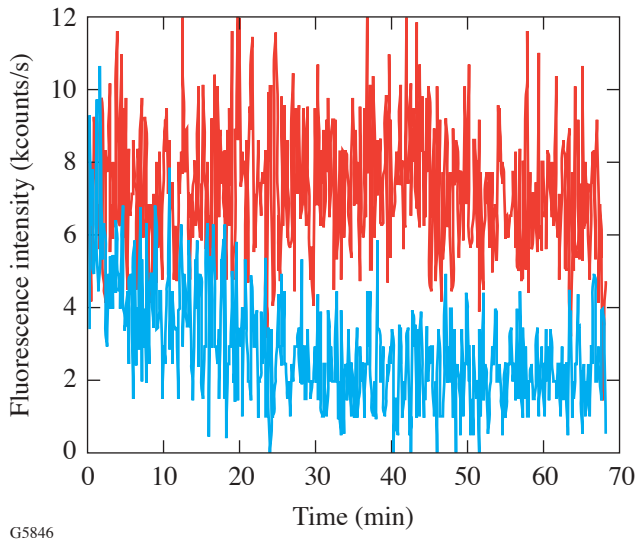

Figure 94.37
Fluorescence bleaching behavior of an assembly of terrylene molecules as a function of time and in two different liquid crystal hosts.

Dye bleaching is not a critical impairment for an efficient SPS, but it is an important factor for device simplicity and cost. When one molecule is bleached, the system can be rapidly realigned to utilize another isolated dye molecule, allowing practically continuous source action (see left histograms on Figs. 94.34–94.36).

Both well-known liquid crystal hosts are photochemically stable and do not absorb excitation light. In addition, incident intensities are too low for two-photon absorption processes. The absorption by a single molecule is insufficient for significant host heating.

Conclusion

A robust, room-temperature single-photon source based on fluorescence from a single dye molecule (fluorescence antibunching) was demonstrated for the first time for liquid crystal hosts. Planar-aligned, 1-D photonic-band-gap structures in dye-doped cholesteric oligomer were prepared. Avoiding bleaching of the terrylene dye molecules for excitation times >1 h was achieved by innovative preparation procedures. Liquid crystal hosts further increase the efficiency of the source (1) by aligning the dye molecules along a direction preferable for maximum excitation efficiency; and (2) by tuning a 1-D photonic-band-gap microcavity of planar-aligned cholesteric liquid crystal to the dye fluorescence band. Source-efficiency issues will be addressed in a subsequent article.

Future work will be directed toward increasing the efficiency, life, and polarization purity of the single-photon source by improved selection of dye, liquid crystal, and the photonic-band-gap structure matching with the dye-fluorescence band. A pulsed laser source will be used to create a real quantum cryptography system with a cholesteric-liquid-crystal, single-photon source on demand.

ACKNOWLEDGMENT

The authors acknowledge the support by the U.S. Army Research Office under Award No. DAAD19-02-1-0285. The work was also supported by the U.S. Department of Energy Office of Inertial Confinement Fusion under Cooperative Agreement No. DE-FC03-92SF19460, the University of Rochester, and the New York State Energy Research and Development Authority. The support of DOE does not constitute an endorsement by DOE of the views expressed in this article. Receipt of OCLC starting material from Dr. F. Kreuzer of Wacker, Munich, is gratefully acknowledged. The authors thank L. Novotny, K. Marshall, J. Shojaie, O. Hollricher, and T. Kosc for advice and help, J. Howell and D. A. Voloshchenko for fruitful discussions, S. Papernov for help with AFM imaging of OCLC, and J. Starowitz for help in the Optical Materials Laboratory.

REFERENCES

1. M. A. Nielsen and I. L. Chuang, *Quantum Computation and Quantum Information* (Cambridge University Press, Cambridge, England, 2001).
2. J. Gruska, *Quantum Computing*, Advanced Topics in Computer Science Series (McGraw-Hill, London, 1999).
3. M. Brooks, ed. *Quantum Computing and Communications* (Springer, London, 1999).
4. C. P. Williams and S. H. Clearwater, *Explorations in Quantum Computing* (TELOS, Santa Clara, CA, 1998).
5. D. Deutsch, *The Fabric of Reality* (Penguin, London, 1998); T. Siegfried, *The Bit and The Pendulum: From Quantum Computing to M Theory—The New Physics of Information* (Wiley, New York, 2000).
6. S. Singh, *The Code Book: The Science of Secrecy from Ancient Egypt to Quantum Cryptography* (Anchor Books, New York, 2000).
7. J. R. Brown, *Minds, Machines, and Multiverse: The Quest for the Quantum Computer* (Simon & Schuster, New York, 2000).
8. P. Kumar, G. M. D'Ariano, and O. Hirota, eds. *Quantum Communication, Computing and Measurement 2* (Kluwer Academic/Plenum Publishers, New York, 2000).
9. D. Bouwmeester, A. K. Ekert, and A. Zeilinger, eds. *The Physics of Quantum Information: Quantum Cryptography, Quantum Teleportation, Quantum Computation*, 1st ed. (Springer, Berlin, 2000).
10. H.-K. Lo, T. Spiller, and S. Popescu, eds. *Introduction to Quantum Computation and Information* (World Scientific, Singapore, 1998).
11. S. L. Braunstein, *Quantum Computing: Where Do We Want to Go Tomorrow?* (Wiley-VCH, Weinheim, 1999).
12. S. L. Braunstein, H.-K. Lo, and K. Pieter, *Scalable Quantum Computers: Paving the Way to Realization*, 1st ed. (Wiley-VCH, Berlin, 2001).
13. G. J. Milburn, *The Feynman Processor: Quantum Entanglement and the Computing Revolution*, Frontiers of Science (Perseus Books, Reading, MA, 1998).
14. N. Gisin *et al.*, Rev. Mod. Phys. **74**, 145 (2002); S. Ya. Kilin, Usp. Fiz. Nauk **42**, 435 (1999).
15. A. Steane, Rep. Prog. Phys. **61**, 117 (1998).
16. D. Aharonov, in *Annual Reviews of Computational Physics. VI*, edited by D. Stauffer (World Scientific, Singapore, 1999), pp. 259–346.
17. A. Galindo and M. A. Martin-Delgado, Rev. Mod. Phys. **74**, 347 (2002).
18. D. P. DiVincenzo, Science **270**, 255 (1995).
19. A. K. Ekert and R. Jozsa, Rev. Mod. Phys. **68**, 733 (1996).
20. J. Preskill, Course information for Physics 219/Computer Science 219 available at http://theory.caltech.edu/~preskill/ph229 (California Institute of Technology, Pasadena, CA, 2000).
21. A. Y. Kitaev, Russ. Math. Surv. **52**, 1191 (1997).
22. The Center for Quantum Computation (Oxford) (http://www.qubit.org).
23. The International Conference on Quantum Information (ICQI) and the Eighth Rochester Conference on Coherence and Quantum Optics (CQO8) Rochester, NY, 10–16 June 2001; see http://www.optics.rochester.edu/~stroud/conference.
24. G. Giedke, "What is Quantum Information Processing?," available at www.magiqtech.com/products/whatisqip.php.
25. P. L. Knight and R. W. Boyd, eds., J. Mod. Opt. (Special Issue: Quantum Communication) **41** (12) (1994); G. Rarity, P. R. Tapster, and P. M. Gorman, eds., J. Mod. Opt. (Special Issue: Technologies for Quantum Communications) **48** (13) (2001); P. G. Kwiat, ed., New J. Phys. (Focus on Quantum Cryptography) **4** (2002).

26. S. Braunstein and H.-K. Lo, eds., Fortschr. Phys. (Special Focus Issue: Experimental Proposals for Quantum Computation) **48** (9–11) (2000).

27. I. Chuang, Nature **420**, 25 (2002); Quantum Information and Computation **1** (1) (2001).

28. C. H. Bennett, Phys. Today **48**, 24 (1995).

29. I. Walmsley and P. Knight, Opt. Photonics News, November 2002, 42.

30. W. P. Risk and D. S. Bethune, Opt. Photonics News, July 2002, 26.

31. A. Zeilinger, Phys. World **11**, 35 (1998).

32. M. A. Nielsen, Sci. Am. **287**, 67 (2002).

33. See http://www.sciam.com for Scientific American articles related to quantum information science.

34. J. A. Wheeler and W. H. Zurek, eds. *Quantum Theory and Measurement*, Princeton Series in Physics (Princeton University Press, Princeton, NJ, 1983).

35. P. Jonsson, "Generation, Detection and Applications of Single Photons," Ph.D. thesis, Royal Institute of Technology, 2002; "Solid State Sources for Single Photons (S4P)," available at http://www.iota.u-psud.fr/~S4P/.

36. D. F. Walls and G. J. Milburn, *Quantum Optics* (Springer-Verlag, Berlin, 1995), p. 42.

37. L. Davidovich, Rev. Mod. Phys. **68**, 127 (1996).

38. U. Mets, in *Fluorescence Correlation Spectroscopy: Theory and Applications*, edited by R. Rigler and E. Elson, Springer Series in Chemical Physics, Vol. 65 (Springer, Berlin, 2001), pp. 346–359.

39. R. J. Hughes, G. L. Morgan, and C. G. Peterson, J. Mod. Opt. **47**, 533 (2000); R. J. Hughes *et al*., New J. Phys. **4**, 43 (2002); J. G. Rarity *et al*., New J. Phys. **4**, 82 (2002).

40. D. Stucki *et al*., New J. Phys. **4**, 41 (2002); E. Klarreich, Nature **418**, 270 (2002).

41. A. V. Sergienko *et al*., Phys. Rev. A **60**, R2622 (1999); B. C. Jacobs and J. D. Franson, Opt. Lett. **21**, 1854 (1996).

42. E. Knill, R. Laflamme, and G. J. Milburn, Nature **409**, 46 (2001); E. Knill, R. Laflamme, and G. Milburn, "Efficient Linear Optics Quantum Computation" (2000), available at http://arXiv.org/abs/quant-ph/0006088.

43. J. Calsamiglia, "Quantum Information Processing and Its Linear Optical Implementation," Ph.D. thesis, University of Helsinki, 2001.

44. Q. A. Turchette *et al*., Phys. Rev. Lett. **75**, 4710 (1995).

45. C. K. Law, J. Mod. Opt. **44**, 2067 (1997).

46. N. J. Cerf, C. Adami, and P. G. Kwiat, Phys. Rev. A **57**, R1477 (1998).

47. J. C. Howell and J. A. Yeazell, Phys. Rev. Lett. **75**, 198 (2000).

48. *Ibid*., Phys. Rev. A **61**, 052303 (2000).

49. *Ibid*., 012304 (2000).

50. T. B. Pittman, B. C. Jacobs, and J. D. Franson, Phys. Rev. Lett. **88**, 257902 (2002).

51. *Ibid*., Phys. Rev. A **64**, 062311 (2001).

52. A. Shields, Science **297**, 1821 (2002).

53. S. Benjamin, Science **290**, 2273 (2000).

54. H. J. Kimble, M. Dagenais, and L. Mandel, Phys. Rev. Lett. **39**, 691 (1977).

55. C. K. Hong and L. Mandel, Phys. Rev. Lett. **56**, 58 (1986).

56. F. Diedrich and H. Walther, Phys. Rev. Lett. **58**, 203 (1987).

57. P. Grangier, G. Roger, and A. Aspect, Europhys. Lett. **1**, 173 (1986).

58. W. P. Ambrose *et al*., Chem. Phys. Lett. **269**, 365 (1997).

59. C. Kurtsiefer *et al*., Phys. Rev. Lett. **85**, 290 (2000).

60. R. Brouri *et al*., Opt. Lett. **25**, 1294 (2000).

61. S. Mayer, "N/V-Zentren als Einzel-Photonen-Quelle," Ph.D. thesis, Ludwig-Maximilians-Universität München, 2000.

62. L. Fleury *et al*., Phys. Rev. Lett. **84**, 1148 (2000).

63. F. Treussart *et al*., Opt. Lett. **26**, 1504 (2001).

64. F. De Martini, G. Di Giuseppe, and M. Marrocco, Phys. Rev. Lett. **76**, 900 (1996).

65. J. Kim *et al*., Nature **397**, 500 (1999).

66. A. Imamoglu and Y. Yamamoto, Phys. Rev. Lett. **72**, 210 (1994).

67. E. Moreau *et al*., Appl. Phys. Lett. **79**, 2865 (2001).

68. P. Michler *et al*., Science **290**, 2282 (2000).

69. C. Santori *et al*., Phys. Rev. Lett. **86**, 1502 (2001).

70. J. Hecht, Laser Focus World **38**, 20 (2002).

71. Z. Yuan *et al*., Science **295**, 102 (2001).

72. C. Brunel *et al*., Phys. Rev. Lett. **83**, 2722 (1999).

73. B. Lounis and W. E. Moerner, Nature **407**, 491 (2000).

74. F. Treussart *et al*., Phys. Rev. Lett. **89**, 093601 (2002).

75. A. Beveratos *et al*., Eur. Phys. J. D **18**, 191 (2002).

76. A. Beveratos *et al*., Phys. Rev. Lett. **89**, 187901 (2002).

77. P. Michler *et al*., Nature **406**, 968 (2000).

78. B. Lounis *et al*., Chem. Phys. Lett. **329**, 399 (2000).

79. G. Messin *et al*., Opt. Lett. **26**, 1891 (2001).

80. T. Basché *et al*., eds. *Single-Molecule Optical Detection, Imaging and Spectroscopy* (VCH Publishers, Weinheim, 1997).

81. W. E. Moerner and M. Orrit, Science **283**, 1670 (1999).

82. W. E. Moerner, Science **277**, 1059 (1997).

83. T. Basché *et al*., Phys. Rev. Lett. **69**, 1516 (1992).

84. L. Fleury *et al*., Mol. Phys. **95**, 1333 (1998).

85. F. Kulzer *et al*., Chem. Phys. **247**, 23 (1999).

86. S. Chandrasekhar, *Liquid Crystals*, Cambridge Monographs on Physics (Cambridge University Press, Cambridge, England, 1977).

87. E. Yablonovitch, Phys. Rev. Lett. **58**, 2059 (1987).

88. S. John, Phys. Rev. Lett. **58**, 2486 (1987).

89. E. Yablonovitch, J. Opt. Soc. Am. B **10**, 283 (1993).

90. P. R. Villeneuve and M. Piché, Prog. Quantum Electron. **18**, 153 (1994).

91. G. Kurizki and J. W. Haus, eds., J. Mod. Opt. (Special Issue: Photonic Band Structures) **41** (2) (1994).

92. S.-H. Chen, D. Katsis, A. W. Schmid, J. C. Mastrangelo, T. Tsutsui, and T. N. Blanton, Nature **397**, 506 (1999).

93. D. Katsis, A. W. Schmid, and S.-H. Chen, Liq. Cryst. **26**, 181 (1999).

94. T. J. Bunning and F. H. Kreuzer, Trends Polym. Sci. **3**, 318 (1995).

95. V. I. Kopp *et al*., Opt. Lett. **23**, 1707 (1998).

96. I. P. Il'chishin *et al*., JETP Lett. **32**, 24 (1980).

97. B. Taheri *et al*., Mol. Cryst. Liq. Cryst. **358**, 73 (2001).

98. H. Finkelmann *et al*., Adv. Mater. **13**, 1069 (2001).

99. O. D. Lavrentovich and M. Kleman, in *Chirality in Liquid Crystals*, edited by H.-S. Kitzerow and C. Bahr, Partially Ordered Systems (Springer, New York, 2001), pp. 115–158.

100. L. Ramos *et al*., Phys. Rev. E **66**, 031711 (2002).

101. Y. Geng, A. Trajkovska, D. Katsis, J. J. Ou, S. W. Culligan, and S. H. Chen, J. Am. Chem. Soc. **124**, 8337 (2002).

102. R. Hanbury Brown and R. Q. Twiss, Nature **177**, 27 (1956).

103. A. Molski, Chem. Phys. Lett. **324**, 301 (2000).